Effects of moderate X-ray Solar flares observed on VLF signals with relatively short GCPs

Aleksandra Kolarski

Technical faculty "Mihajlo Pupin", University of Novi Sad, Zrenjanin, Serbia

Abstract

Solar electromagnetic energy of wavelength range 0.1-0.8 nm, emitted during occurrence of Solar flare events and often called soft X-ray radiation, penetrates deep into the Earth′s atmosphere, where causes abrupt and intense changes of ionized medium within altitude range 50-90 km that corresponds to lower Ionosphere. D-region is used by Very Low Frequency (VLF) radio signals for their transmission, so their propagation parameters are highly sensitive to related sudden environmental plasma changes due to incident Solar flare energy. Effects of Solar flare events of moderate intensity of C and M class were analyzed on VLF data recorded by narrowband recording system located in Belgrade, Serbia, at the Institute of Physic (44.85N, 20.38W). Time span for analysis encompasses VLF data registered during the second half of the 23rd Solar cycle, mainly in period from 2004 to 2008. Solar flare signature analysis had focus on VLF signals of relatively short paths and included GQD/22.1 kHz, DHO/23.4 kHz, HWU/18.3 kHz and ICV/20.27 kHz signals, emitted from European military transmitters located in UK, Germany, France and Italy, respectively, and registered in Belgrade during inspected time period. Time evolution of flare induced series of perturbations, with accompanying related propagation parameters′ deviations from their regulars, was inspected in detail. For lower Ionospheric plasma environment modeling, Long Wave Propagation Capability (LWPC) software, both for regular and perturbed ionization states, was applied. Main results are presented in this paper.

Key words: Solar flare, VLF signal, lower Ionosphere, perturbation, density change, D-region.

Introduction

Sudden outbursts of electromagnetic energy emitted from Sun within wavelength range 0.1-0.8 nm (soft X-ray radiation) abruptly change properties of ionized medium originating in sunlit Earth′s atmosphere, at Ionospheric D-region altitudes 50-90 km [1]. SubIonospheric propagation of Very Low Frequency (VLF)

radio signals (3-30 kHz) is highly sensitive to sudden environmental plasma changes in lower Ionosphere induced by incident Solar flare energy. VLF signals globally transmitting with stable propagation (e.g. [2-4]) are commonly used as the tool for remote sensing of the lower Ionosphere, for vast range of forcing agents of extraterrestrial and terrestrial origin. Variety of different aspects is covered in numerous manuscripts (review of relatively recent results is summarized in e.g. [5] and references therein). In this paper, VLF technique is used for analysis of effects of X-ray Solar flares of moderate intensity on the lower Ionosphere, based on VLF signal propagation.

VLF data used in this research were taken from database of VLF radio signals of The Absolute Phase and Amplitude Logger (AbsPAL) narrowband receiving system, operating at the Institute of Physics in Belgrade (44.85N, 20.38W), Serbia. Research focus was VLF signals of relatively short Great Circle Paths (GCPs) under influence of Solar flare radiation of moderate intensity in soft X-range. Solar flare events, from the second half of 23rd Solar cycle and their signatures on VLF signals were examined, with aim to determine lower Ionospheric plasma characteristics affected by C and M class Solar flares, as deduced from VLF data registered in Belgrade.

For modeling purposes of lower Ionospheric conditions, before, under perturbations induced by Solar flare events and after that influence, procedure for simulation of subIonospheric propagation of VLF signals incorporated within Long Wave Propagation Capability (LWPC) [6] software was used. The outline of LWPC software is propagation of VLF signals in stratified medium implying exponential conductivity increase with height within incorporated Ionospheric model, with propagation of VLF signals described by hop wave theory (e.g. [7, 8]) and Earth-Ionosphere waveguide with its upper boundary defined by the lower edge of the Ionosphere and its lower boundary defined by Earth′s surface based upon real globally measured values of electro-conductivity. Propagation model [9] is defined by the electron density Ne (m^{-3}) within the waveguide at the altitude z (km), as described by parameter pairs denoted reflecting edge *sharpness* β (km^{-1}) of the lower Ionospheric boundary and *reflecting height* H′ (km). Wait′s theory defines Ne (m^{-3}) through relation designed for daytime Ionospheric conditions as:

$$Ne(z, H', \beta) = 1.43 \cdot 10^{13} \cdot e^{-0.15H'} \cdot e^{(\beta-0.15)(z-H')}. \quad (1)$$

As the output, program gives calculated amplitude and phase delay based on propagation simulation of defined VLF signal along chosen path, taking into account the whole range of parameters as background data (such as signal frequency, bearing angle, receiver and transmitter locations, observed date and time, solar zenith angle, geomagnetic dip, electro-conductivity of lower waveguide boundary etc). Proposed model within LWPC software package, in case of daytime unperturbed regular Ionospheric conditions, takes (β, H′) parameter pair defined as (0.3, 74), but for modeling purposes it is necessary manually to input into the

software wanted parameter pairs (β, H') in order to model just segment of the path or the whole path entirely, depending of conducted calculations′ complexity.

Analysis and results

Belgrade AbsPAL station works in fully operational mode since 2004, although there are also some registrations during the last trimester of 2003. During inspected period, several VLF signals were registered: NAA/24.0 kHz emitted from USA, GQD/22.1 kHz from UK, NWC/19.8 kHz from Australia, DHO/23.4 kHz from Germany, ICV/20.27 kHz from Italy, HWU/18.3 kHz from France and also from some other transmitters, but the latter in short time segments and usually not with good data quality. In general, long GCP NAA/24.0 kHz and NWC/19.8 kHz signals (about 6.5 Mm and near 12 Mm, respectively), and short GCP GQD/22.1 kHz signal (near 2 Mm), were registered continually and usually with good quality data. Among other short GCP signals, there were often alterations, but mostly were registered HWU/18.3 kHz (near 1.5 Mm), DHO/23.4 kHz signals (1.3 Mm) and ICV/20.27 kHz (near 1 Mm). VLF signals registered by Belgrade AbsPAL receiver during period 2004-2009 are given in Fig. 1. Characteristics of VLF transmitters

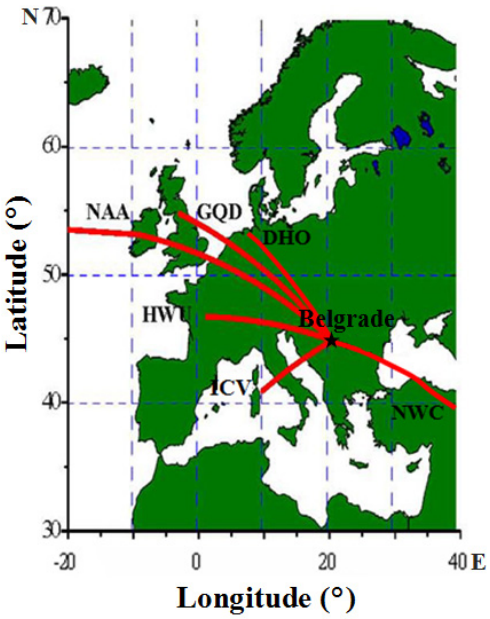

Fig. 1. VLF signals (in red) registered in Belgrade (star) by AbsPAL receiver in period 2004-2009

Table 1. VLF transmitters (T_x) and VLF signals registered in Belgrade during analyzed period

VLF signal (kHz)	T_x location	T_x power (kW)	GCP (km)
NAA/24.0	Maine, USA (44.63N; 67.28W)	1000	6547
GQD/22.1	Skelton, UK (54.72N; 2.88W)	300	1982
NWC/19.8	H. E. Holt, Australia (27.2S; 114.98E)	1000	11975
DHO/23.4	Rhauderfehn, Germany (53.08N; 7.62E)	800	1301
ICV/20.27	Isola di Tavolara, Italy (NATO) (40.92N; 9.73E)	20	970
HWU/18.3	Rosnay, France (NATO) (46.71N; 1.24E	400	1493

and Great Circle Path (GCP) length of VLF signals registered in Belgrade during the analyzed period are given in Table 1.

Analysis was conducted for short path VLF signals, with GQD signal depicted in detail. Examples of monitored Solar flare signatures on GQD signal, during two very active days and some representative examples of recorded VLF perturbations, induced by Solar flare events of moderate intensity within period of interest, are given in Fig. 2. Detailed analysis of GQD signal amplitude and phase delay perturbations induced by selected C and M class flare events, from period December 2005 – July 2006 (Table 2 and Fig. 3) was carried out, with corresponding propagation parameters′ modeling procedure conducted throughout the entire time evolution of inducing X-ray Solar irradiances, implemented by utilization of Long Wave Propagation Capability (LWPC) numeric routine code for modeling VLF subIonospheric propagation. GQD signal amplitude and phase delay perturbation, induced by shown flare events, differ in patterns between one another, due to diurnal and seasonal propagation factors and also due to different time evolution of selected flares, but in general have oscillatory character, which is characteristic feature for this signal as registered in Belgrade [10, 11]. Sluggishness of the Ionosphere [12, 13] in analyzed cases is of absolute amount up to 2 min, for main signal extremum, both in case of amplitude (D_A) and phase delay (D_P) [12, 14].

Table 2. Flare events of moderate intensity which effects were inspected on analyzed GQD/22.1 kHz signal

date (dd-mm-yy)	Ix_{max} time (UT)	flare class	Ix_{max} (Wm^{-2})	D_A (min)	D_P (min)	quiet day (dd-mm-yy)	preflare state in waveguide
07-04-06	08:03	C9.7	$9.74 \cdot 10^{-6}$	1	2	08-04-06	regular
06-07-06	08:36	M2.5	$2.51 \cdot 10^{-5}$	1	-2	05-07-06	regular
06-12-06	12:58	C4.8	$4.82 \cdot 10^{-6}$	1	1	08-12-06	perturbed
07-09-05	12:44	C9.6	$9.62 \cdot 10^{-6}$	2	0	08-09-05	perturbed

Regular (A_{reg}, P_{reg}) and perturbed (A_{flare}, P_{flare}) VLF data were directly obtained from VLF recordings, by reading these values from registered GQD signals in Belgrade. Difference between measured perturbed and regular values (ΔA and ΔP) was calculated by simple subtraction of regular from perturbed values, i.e. as $\Delta A = A_{flare} - A_{reg}$ and $\Delta P = P_{flare} - P_{reg}$). All these data were used as an input data, for conducted modeling procedure by means of LWPC program, when defining input parameter pairs (β, H') in REXP subroutine. Modeling of lower Ionospheric properties under influence of selected moderate flare events was designed in that manner, primarily to get modeled pair of values (ΔA_m and ΔP_m), but also modeled values of amplitude (A_m, both regular and perturbed) and phase delay (P_m, both regular and perturbed), as close as possible to real measured data red from registered signals. In this way, simulated signal propagation conditions, both in unperturbed state and under influence of flare, can be considered to appropriately depict real propagation in Earth-ionsphere waveguide. Modeling procedure itself consists of numerous trial and error iterations applied until desired accuracy of output results (ΔA_m, ΔP_m, A_m and P_m) is achieved (here, within 10-20%). Based on the modeled parameters (β, H') obtained from simulations as final best fitting pair, electron density height profile is calculated using relation (1).

On one hand, modeling either can be performed for some chosen characteristic moments during the influence of Solar X-radiation, depending on signal′s perturbation pattern features and complexity, or for entire time evolution of Solar flare event and on the other hand, modeled values of electron density within altitude range corresponding to sunlit D-region either can be calculated for some chosen heights, or throughout the entire altitude range. In case of VLF signals of short GCPs, when entirely sunlit, propagation within entire waveguide can be

described with single pair of (β, H′), depicting average conditions along signal trace during modeling. In this paper, modeling was performed for entire time interval during the influence of chosen flare events onto the GQD signal and for the entire altitude range of heights from 50 to 90 km. For the sake of visibility, only characteristic moments (marked with arrows in Fig. 3) and corresponding electron density variations (Fig. 4) are presented here, with some chosen parameters listed in Table 3 (e.g. Ne (60 and 85 km) (m^{-3})) .

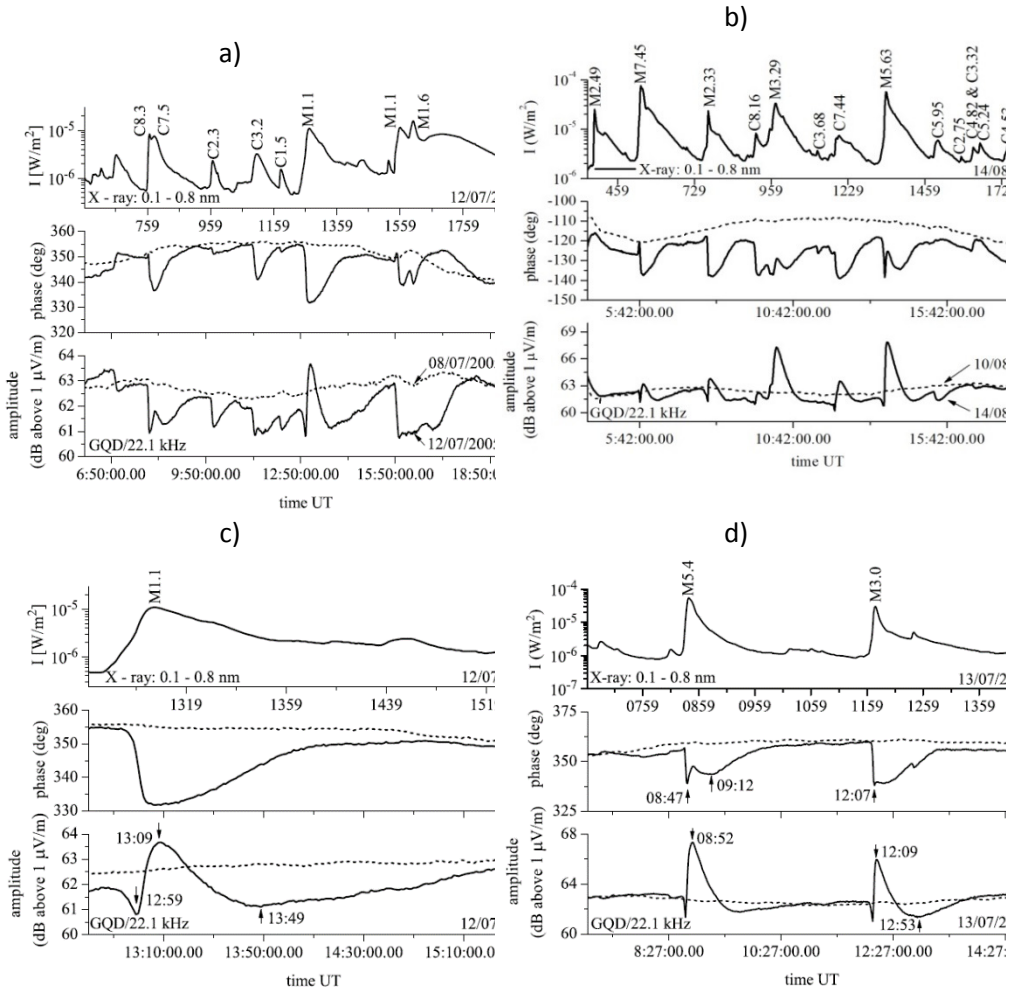

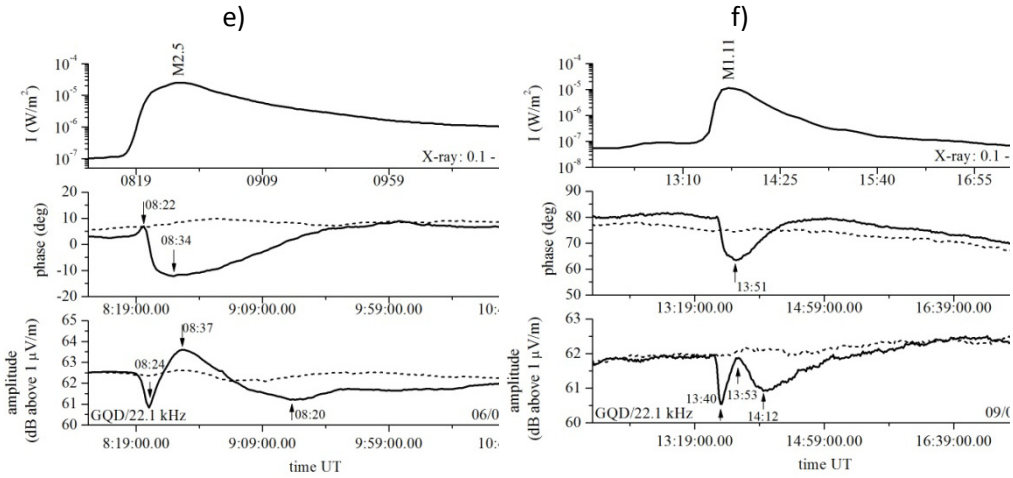

Fig. 2. GQD signal amplitude and phase delay perturbations (lower and middle panels – solid lines) induced by Solar flare events of moderate intensity (X-ray irradiance - upper panels): a) during very active periods on 12th July, 2005 (quiet day 08th July, 2005 – dashed lines) and b) 14th August, 2004 (quiet day 10th August, 2004), and by c) M1.1 Solar flare occurred at 13:06UT on 12th July, 2005 (quiet day 08th July, 2005), d) M5.4 and M3.0 Solar flares occurred at 08:48UT and 12:08UT respectively on 13th July, 2004 (quiet day 08th July, 2005), e) M2.5 Solar flare occurred at 08:36UT on 06th July, 2006 on the left (quiet day 05th July, 2006) and f) M1.11 Solar flare occurred at 13:48Ut on 09th June, 2007 on the right (quiet day 10th June, 2007); signal extrema are indicated by arrows and time UT.

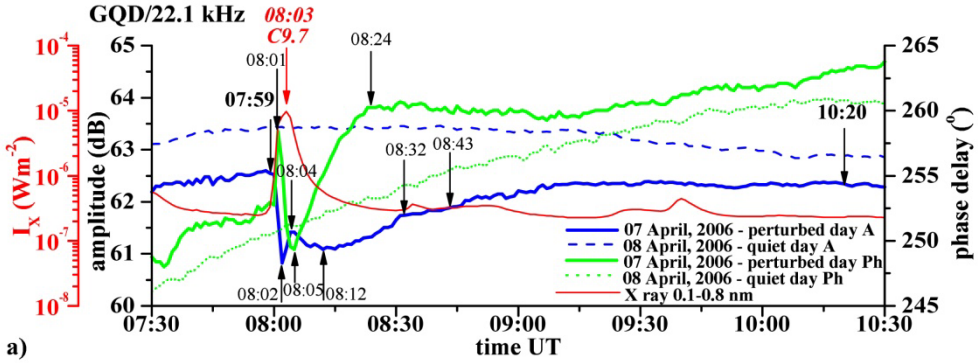

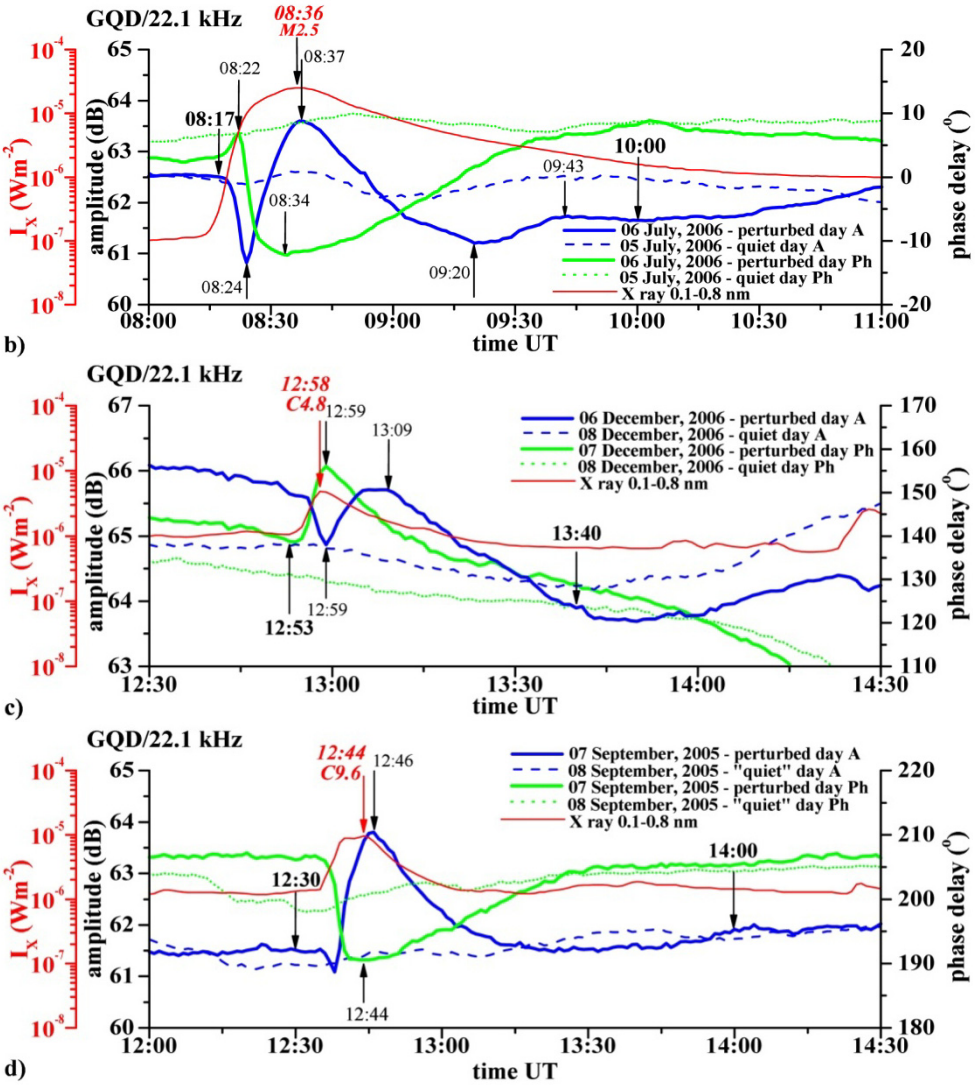

Fig. 3. Variation of GQD signal forced by Solar flares of moderate intensity (red thin solid lines) from 2005-2006: a) C9.7 (08:03UT) flare event occurred on 07th April, 2006, b) M2.5 (08:36UT) on 06th July, 2006, c) C4.8 (12:58UT) on 06th December, 2006 and d) C9.6 (12:44UT) on 07th September, 2005; perturbed signal amplitude and phase delay – blue and green thick solid lines, respectively; regular signal amplitude and phase delay – blue dashed and green dotted lines; signal extrema indicated by black arrows and time UT, while flare event in red.

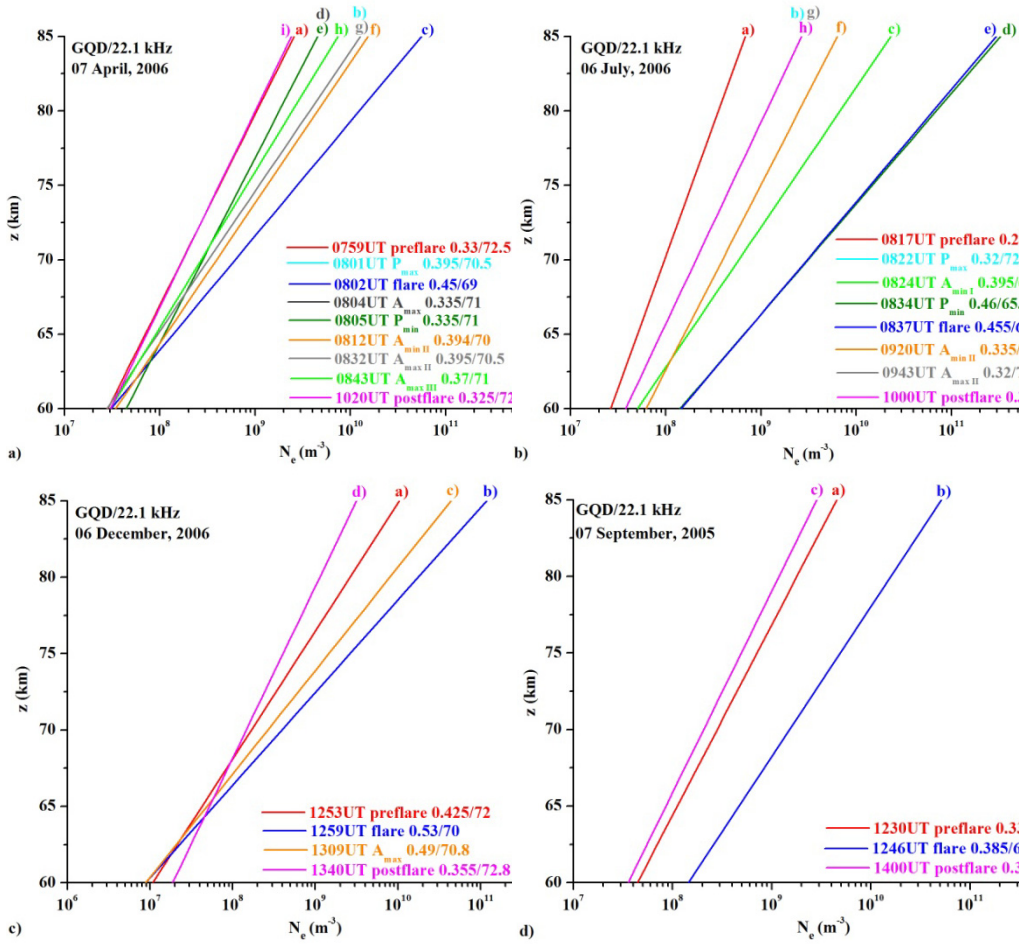

Fig. 4. Electron density height profile variations within D-region, corresponding to induced Ionosation changes under considered Solar flare events of moderate intensity: a) C9.7 (08:03UT) flare event occurred on 07th April, 2006, b) M2.5 (08:36UT) on 06th July, 2006, c) C4.8 (12:58UT) on 06th December, 2006 and d) C9.6 (12:44UT) on 07th September, 2005; preflare Ionospheric state is indicated in red, state that corresponds to Ix_{max} irradiance is given in blue and posltflare state in pink; for striking signal extrema indicated by black arrows accompanied signal state and parameter pairs (β, H′) are shown.

Electron densities estimated by similar modeling procedure at height 74 km (Table 3), although conducted for several moments during time evolution of analyzed flare events is presented in [15] with electron density height profiles modeled for preflare, flare and postflare GQD signal states. Also, some additional information on Ne (m^{-3}) at D-region boundaries at altitudes 50 and 90 km for preflare, flare and postflare GQD signal states, with some Ionospheric plasma

behavior comparisons in case of long NAA path, as registered by Belgrade AbsPAL VLF receiver during considered flare events, can be found in [16]. In present research, modeling procedure was conducted for entire time evolution of considered Solar flare events, with electron density height profile variations estimated within entire altitude range that corresponds to lower Ionosphere D-region (50-90 km).

Table 3. Parameters characterizing GQD/22.1 kHz signal propagation conditions under influence of considered X-ray Solar flare events of moderate intensity

flare date (dd-mm-yy) timeUT	time (UT)	signal state	ΔA (dB)	ΔP (o)	β (km^{-1})	H′ (km)	Ne (m^{-3})		
							74 km [15]	60 km	85 km
	07:59	preflare	-0.89	2.52	0.33	72.5	$3.54\cdot10^{8}$	$2.85\cdot10^{7}$	$2.57\cdot10^{9}$
	08:01	P_{max}	-1.72	7.68	0.395	70.5	$8.61\cdot10^{8}$	$2.79\cdot10^{7}$	$1.27\cdot10^{10}$
	08:02	flare	-2.62	4.93	0.45	69	$2.05\cdot10^{9}$	$3.07\cdot10^{7}$	$5.56\cdot10^{10}$
07-04-06	08:04	A_{max1}	-1.98	-1.69	0.335	71	$5.90\cdot10^{8}$	$4.43\cdot10^{7}$	$4.52\cdot10^{9}$
08:03UT	08:05	P_{min}	-1.99	-1.78	0.335	71	$5.90\cdot10^{8}$	$4.43\cdot10^{7}$	$4.52\cdot10^{9}$
C9.7	08:12	A_{min2}	-2.34	3.09	0.394	70	$1.04\cdot10^{9}$	$3.43\cdot10^{7}$	$1.53\cdot10^{10}$
	08:32	A_{max2}	-1.71	6.28	0.395	70.5	$8.61\cdot10^{8}$	$2.79\cdot10^{7}$	$1.27\cdot10^{10}$
	08:43	A_{min3}	-1.55	4.48	0.37	71	$6.56\cdot10^{8}$	$3.01\cdot10^{7}$	$7.37\cdot10^{9}$
	10:20	postflare	-0.53	2.31	0.325	72.5	$3.52\cdot10^{8}$	$3.04\cdot10^{7}$	$2.41\cdot10^{9}$
	08:17	preflare	0.04	-3.44	0.28	75	$1.63\cdot10^{8}$	$2.65\cdot10^{7}$	$6.82\cdot10^{8}$
	08:22	P_{max}	-0.72	0.11	0.32	72	$4.10\cdot10^{8}$	$3.79\cdot10^{7}$	$2.66\cdot10^{9}$
06-07-06	08:24	A_{min1}	-1.54	-6.46	0.395	69	$1.56\cdot10^{9}$	$5.04\cdot10^{7}$	$2.31\cdot10^{10}$
08:36UT	08:34	P_{min}	0.76	-20.34	0.46	65.5	$1.08\cdot10^{10}$	$1.41\cdot10^{8}$	$3.26\cdot10^{11}$
M2.5	**08:37**	flare	1.0	-20.25	0.455	65.5	$1.03\cdot10^{10}$	$1.44\cdot10^{8}$	$2.96\cdot10^{11}$
	09:20	A_{min2}	-1.11	-6.54	0.335	70	$8.25\cdot10^{8}$	$6.19\cdot10^{7}$	$6.32\cdot10^{9}$
	09:43	A_{max2}	-0.79	-0.99	0.32	72	$4.10\cdot10^{8}$	$3.79\cdot10^{7}$	$2.66\cdot10^{9}$
	10:00	postflare	-0.79	-0.44	0.32	72	$4.10\cdot10^{8}$	$3.79\cdot10^{7}$	$2.66\cdot10^{9}$
06-12-06	**12:53**	preflare	0.8	7.44	0.425	72	$5.06\cdot10^{8}$	$1.08\cdot10^{7}$	$1.04\cdot10^{10}$
12:58UT	**12:59**	flare	0.06	26.71	0.53	70	$1.80\cdot10^{9}$	$8.81\cdot10^{6}$	$1.18\cdot10^{11}$
C4.8	13:09	A_{max}	1.09	15.41	0.49	70.8	$1.04\cdot10^{9}$	$8.88\cdot10^{6}$	$4.36\cdot10^{10}$
	13:40	postflare	-0.33	5.51	0.355	72.8	$3.31\cdot10^{8}$	$1.88\cdot10^{7}$	$3.16\cdot10^{9}$
07-09-05	**12:30**	preflare	0.29	2.09	0.355	71	$5.90\cdot10^{8}$	$4.43\cdot10^{7}$	$4.52\cdot10^{9}$
12:44UT	**12:46**	flare	2.32	-13.33	0.385	66.5	$3.88\cdot10^{9}$	$1.44\cdot10^{8}$	$5.14\cdot10^{10}$
C9.6	**14:00**	postflare	0.19	1.36	0.325	72	$4.14\cdot10^{8}$	$3.57\cdot10^{7}$	$2.84\cdot10^{9}$

Discussion and conclusions

Propagation model based on Wait′s parameters and LWPC calculations can be used for VLF signal subionospheric propagation simulations both for unperturbed conditions [14, 17-19] and perturbed conditions due to Solar flare events. Complexity of D-region response to incident X-ray radiation from Sun and variation of Solar flare events′ characteristics themselves, is the reason that issue has been treated from many and diverse aspects primarily regarding flare peak irradiance in perturbed state (e.g. [20, 21]), relaxation period (e.g. [22, 23]), different flare classes (e.g. [10, 11, 14-16, 24-29]) and on the other hand mid- (e.g. [30-38]), low-latitude ionopsphere (e.g. [39-41]) etc. In this paper, utilization of LWPC code routine was applied to selected VLF data from second half of the 23rd Solar cycle, mainly from 2004 to 2008, with goal to inspect Solar flare signatures on VLF signals of relatively short paths, emitted from European military transmitters towards Belgrade AbsPAL receiver station.

In case of GQD/21.1 kHz signal, series of perturbations forced by Solar flare events were thoroughly reviewed and inspected in detail throughout entire time evolution of flare influence. Few chosen events are presented in this paper, with corresponding propagation parameters′ variations related to soft X-ray Solar irradiance. The Earth-ionosphere waveguide was modeled during the entire duration of analyzed flare events′ influence on the lower Ionosphere. Results obtained from LWPC software through conducted modeling procedure are in good agreement with real VLF signal measurements. It can be concluded that modeled averaged waveguide states realistically depict real states of the ionospheric plasma environments held in certain time periods along GQD signal path, as perturbed by these flare events, but also in unperturbed preflare and recovered postflare states.

Determining of ionospheric parameters by different methods introduces errors of about one order of magnitude (factor 10) and also, deviations in determining electron concentrations using different models vary for different altitudes. Comparison of results presented here, with published results of other researchers from Belgrade VLF group in first place, and with some other mid-latitude case studies, shows that in case of perturbed flare state related to Ix_{max} electron density ratios are within one order of magnitude compared to values given in [11, 14], while in case of unperturbed flare state electron density ratios are smaller than those given [23]. Electron densities at 74 km altitude are realistic and in line with results given in [14, 21, 34, 35, 43], and electron density height profiles are realistic. Determining ionospheric parameters and electron density height distribution by sophisticated numerical techniques can give more precise results (e.g. [40, 33, 14; 44, 45]), nevertheless, applied Wait theory and LWPC software provide satisfactory modeling results for the purposes of qualitative analysis such as conducted in this paper.

Acknowledgments

Author thanks D. Grubor for help and support in paper preparation and D. Šulić for instrumental set-up. Thanks are due to The Ministry of Education, Science and Technological Development of the Republic of Serbia.

References

1. Whitten, R.C., Poppoff, I.G. (1965) Physics of the Lower Ionosphere. Englewood Cliffs, N.J. Prentice-Hall.
2. Budden, K.G. (1988) The propagation of radio waves. Cambridge University Press, UK.
3. Thomson, N.R. (1993) Experimental daytime VLF ionospheric parameters. *J. Atmos. Sol.-Terr. Phys.* 55 (2), 173–184.
4. McRae, W.M., Thomson, N.R. (2000) VLF phase and amplitude: daytime ionospheric parameters. *J. Atmos. Sol.-Terr. Phys.* 62, 609–618.
5. Silber, I., Price, C. (2017) On the Use of VLF Narrowband Measurements to Study the Lower Ionosphere and the Mesosphere–Lower Thermosphere. *Surveys in Geophysics*. 38(2), 407–441.
6. Ferguson, A.J. (1998) Computer Programs for Assessment of Long-Wavelength Radio Communications, Version 2.0. Technical document 3030. Space and Naval Warfare Systems Center, San Diego CA 92152-5001.
7. Budden, K.G. (1961) The Waveguide Mode Theory of Wave Propagation. Logos Press, London, UK.
8. Wait, R.J. (1970) Electromagnetic Waves in Stratified Media. Pergamon Press, Oxford, UK.
9. Wait, R.J., Spies, K. P. (1964) Characteristics of the Earth-Ionosphere waveguide for VLF radio waves. NBS Technical Note 300, USA.
10. Grubor, D., Šulić, D., Žigman, V. (2005) Influence of Solar x-ray flares on the Earth-ionosphere waveguide. *Serb. Astron. J.* No. 171, 29 – 35.
11. Grubor, D.P., Šulić, D.M., Žigman, V. (2008) Classification of X-ray solar flares regarding their effects on the lower ionosphere electron density profile. *Ann. Geophys.* 26, 1731–1740.
12. Mitra, A.P. (1974) Ionospheric effects of solar flares. Astrophysics and Space Science Library, vol. 46, D. Reidel publishing Company, Boston.
13. Appleton, E.V. (1953) A note on sluggishness of ionosphere. *J. Atmos. Sol.-Terr. Phys.* 3, 282–284.
14. Žigman, V., Grubor, D., Šulić, D. (2007) D-region electron density evaluated from VLF amplitude time delay during X-ray solar flares. *J. Atmos. Sol.-Terr. Phys.* 69, 775–792.
15. Kolarski, A., Grubor, D. (2014) Sensing the Earth's Low Ionosphere during Solar Flares using VLF Signals and GOES Solar X-ray Data. *Adv. Space Res.* 53, 11, pp. 1595 – 1602.

16. Kolarski, A., Grubor, D. (2015) Comparative Analysis of VLF Signal Variation along Trajectory Induced by X-ray Solar Flares. *J. Astrophys. Astr.* Vol. 36, No. 4, pp. 565–579.
17. Thomson, N.R. (1993) Experimental daytime VLF ionospheric parameters. *J. Atmos. Sol.-Terr. Phys.* 55 (2), 173–184.
18. McRae, W.M., Thomson, N.R. (2000) VLF phase and amplitude: daytime ionospheric parameters. *J. Atmos. Sol.-Terr. Phys.* 62, 609–618.
19. Thomson, N.R.; Clilverd, M.A.; Rodger, C.J. (2017) Midlatitude ionospheric D region: Height, sharpness, and solar zenith angle. *J. Geophys. Res. Space.* 122, 8933–8946.
20. Nina, A., Nico, G., Mitrović, S.T., Čadež, V.M., Milošević, I.R., Radovanović, M., Popović, L.Č. (2021) Quiet Ionospheric D-Region (QIonDR) Model Based on VLF/LF Observations. *Remote Sens.* 13, 483.
21. McRae, W.M., Thomson, N.R. (2004) Solar flare induced ionospheric D region enhancements from VLF amplitude observations. *J. Atmos. Sol.-Terr. Phys.* 66, 77–87.
22. Thomson, N.R., Rodger, C.J., Cliverd, M.A. (2005) Large solar flares and their ionospheric D region enhancements. *J. Geophys. Res.* 110, A06306.
23. Nina, A., Čadež, V.M. (2014) Electron Production by Solar Ly-α Line Radiation in the Ionospheric D-region. *Adv. Space Res.* 54, 7, pp. 1276–1284
24. Bajčetić, J., Nina, A., Čadež, V.M., Todorović, B.M. (2015) Ionospheric D-Region Temperature Relaxation and Its Influences on Radio Signal Propagation after Solar X-Flares Occurrence. *Thermal Sci.* 2015, 19, S299–S309.
25. Thomson, N.R., Rodger, C.J., Clilverd, M.A. (2011) Daytime D region parameters from long-path VLF phase and amplitude. *J. Geophys. Res.* 116, 11305–11310.
26. Šulić, D.M., Srećković, V., Mihajlov, A.A. (2016) A study of VLF signals variations associated with the changes of ionization level in the D-region in consequence of solar conditions. *Adv. Space Res.* 57. 1029-1043.
27. Srećković, V.A.; Šulić, D.M.; Ignjatović, L.; Vujčić, V. (2021) Low Ionosphere Under Influence of Strong Solar Radiation: Diagnostics and Modeling. *Appl. Sci.* 11, 7194.
28. Feng, J., Han, B., Gao, F., Zhang, T., Zhao, Z. (2021) Analysis of Global Ionospheric Response to Solar Flares Based on Total Electron Content and Very Low Frequency Signals. *IEEE Access*, vol. 9, pp. 57618-57631.
29. Hayes, L.A., O'Hara, O.S.D., Murray, S.A., Gallagher, P.T. (2021) Solar Flare Effects on the Earth's Lower Ionosphere. *Sol. Phys.* 296, 157.
30. Nina, A., Cadež, V.M., Bajcetic, J., Mitrovic, S.T., Popovic, L.C. (2018) Analysis of the relationship between the solar X-ray radiation intensity and the D-region electron density using satellite and ground-based radio data. *Sol. Phys.* 293, 64.

31. Koen, E.J., Collier, A.B. (2013) Mid-latitude ionospheric signature of a weak solar flare in winter. *S. Afr. j. sci.* vol.109, n.1-2.
32. Bouderba, Y., NaitAmor, S., and Tribeche, M. (2016), Study of the solar flares effect on VLF radio signal propagating along NRK-ALG path using LWPC code, *J. Geophys. Res.* 121, 6799– 6807,
33. Nina, A.; Čadež, V.; Šulić, D.; Srećković, V.; Žigman, V. (2012B) Effective electron recombination coefficient in ionospheric D-region during the relaxation regime after solar flare from 18 February 2011. Nucl. Instrum. *Methods Phys. Res. B* 279, 106–109.
34. Nina, A., Čadež, V., Srećković, V.A., Šulić, D. (2011) The influence of solar spectral lines on electron concentration in terrestrial ionosphere. *Baltic Astron.* 20, 609–612.
35. Kolarski, A., Grubor, D., Šulić, D. (2011) Diagnostics of the solar X-flares impact on the lower ionosphere through the VLF-NAA signal recordings. *Baltic Astron.* 20, 591–595.
36. Šulić, D., Srećković, V. A. (2014) A comparative study of measured amplitude and phase perturbations of VLF and LF radio signals induced by solar flares. *Serb. Astron. J.* 188, 45–54.
37. Todorović Drakul, M., Čadež, V. M., Bajčetić, J. B., Popović, L. Č, Blagojević, D. M., Nina, A. (2016) Behaviour of Electron Content in the Ionospheric D-Region During Solar X-Ray Flares. *Serb. Astron. J.* 193, 11–18.
38. Chakraborty, S., Basak, T. (2020) Numerical analysis of electron density and response time delay during solar flares in mid-latitudinal lower ionosphere. *Astrophys. Space Sci.* 365.
39. Gavrilov, B., Ermak, V., Lyakhov, A. Poklad, Y., Rybakov, V., Ryakhovskiy, I. (2020) Reconstruction of the Parameters of the Lower Midlatitude Ionosphere in M- and X-Class Solar Flares. *Geomagnetism and Aeronomy*, 60. 747-753.
40. Basak, T., Chakrabarti, S.K. (2013) Effective Recombination Coefficient and Solar Zenith Angle Effects on Low-latitude D-region Ionosphere Evaluated from VLF Signal Amplitude and its Time Delay During X-ray Solar Flares. *Astrophys. Space Sci.* 348, 2, pp. 315–326.
41. Pandey, U., Singh, B., Singh, O.P., Saraswat, V.K. (2015) Solar flare induced ionospheric D-region perturbation as observed at a low latitude station Agra, India. *Astrophys Space Sci*. 357:35.
42. Rozhnoi, A., Solovieva, M., Fedun, V., Gallagher, P., McCauley, J., Boudjada, M.Y., Shelyag, S., Eichelberger, H.U. (2019) Strong influence of solar X-ray flares on low-frequency electromagnetic signals in middle latitudes. *Ann. Geophys.* 37, 843–850.
43. Nina, A., Čadež, V., Srećković, V.A., Šulić, D. (2012a) Altitude distribution of electron concentration in ionospheric D-region in presence of timevarying solar radiation flux. *Nucl. Instrum. Methods B* 279, 110–113.

44. Palit, S., Basak, T., Mondal, S.K., Pal, S., Chakrabarti, S.K. (2013) Modeling of very low frequency (VLF) radio wave signal profile due to solar flares using the GEANT4 Monte carlo simulation coupled with ionospheric chemistry. *Atmos. Chem. Phys.* 13, 9159–9168.
45. Tanaka, Y.T. (2010) VLF observations of magnetar flares. *AIP Conf. Proc.* 1286, 331–338.